THE JOURNAL OF PHYSICAL CHEMISTRY Letters

Letter

Cite This: J. Phys. Chem. Lett. 2019, 10, 702−706

pubs.acs.org/JPCL

Ground-State Pd Anions React with H_2 Much Faster than the Excited Pd Anions

Rulin Tang,[†] Xiaoxi Fu,[†] Yuzhu Lu,[†] and Chuangang Ning*[,†,‡]

[†]Department of Physics, State Key Laboratory of Low-Dimensional Quantum Physics, Tsinghua University, Beijing 100084, China

[‡]Collaborative Innovation Center of Quantum Matter, Beijing 100084, China

Supporting Information

ABSTRACT: Recent advances in experimental techniques have made it relatively easy to prepare reactant cations in well-defined states of electronic excitation. Extensive studies on the role of excited states in the cation-neutral reactions have contributed significantly to our understanding of reaction kinetics and dynamics. The excited states are often more reactive than the ground state. However, the reactions involving the excited atomic anion are very rare because the negative ions usually have no bound excited states. In the present work, we report the state-specific reaction of Pd anions with H_2. Surprisingly, we observed that the ground-state Pd anions react with H_2 10 times faster than the excited Pd anions. The high-level calculations show that the difference is due to the reaction barrier.

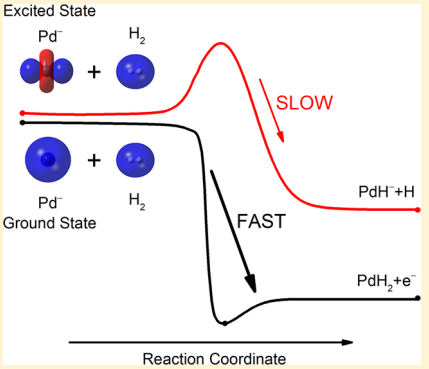

Palladium (Pd) is a unique material with a strong affinity to hydrogen owing to both its catalytic and hydrogen-absorbing properties.[1] Palladium can absorb up to 900 times its own volume of hydrogen at ambient temperature and pressure.[2] It is an important material for hydrogen purification,[3,4] storage,[5] and fuel cells.[6] The interaction of Pd and H_2 has been extensively investigated both experimentally and theoretically.[7−9] In the present work, we report Pd^- reactions with H_2. The negative ions usually have no bound excited states because of the short-range potential between the attached electron and the neutral core. Atomic anions may have bound states with some fine structures due to the spin−orbital coupling effect.[10] The electronic configurations of these fine structures are usually the same. The Pd anion, as a rare exceptional example, has a bound excited state with an electronic configuration different from its ground state. As illustrated in Figure 1, the two bound states are $4d^{10}5s\ ^2S_{1/2}$ for the ground state and $4d^95s^2\ ^2D_{5/2}$ for the excited state. The energy gap between the two states is 1127(4) cm^{-1}.[11] It is an interesting experiment to compare the reactivity of the two states due to the different electronic configurations.

In chemical reactions, the kinetic energies,[12] electronic states,[13] and vibrational states[14] of the reactants can affect the reaction rates, sometimes decisively. The exploration of the different roles of the ground states and the excited states of reactants is helpful for understanding the dynamics of chemical reactions. Some atomic cations can have excited states with a quite long lifetime that can survive from the frequent collisions before the reactions. For example, Armentrout[15−18] and Ng[19−21] have measured the reaction cross sections of some cations (like Cr^{+}[22] and Ar^{+}[23]) at different electronic states with neutral gas. For the $Ni^+ + H_2$ reaction, it was observed that the excited state $4s3d^8\ ^4F$ is less reactive than the ground state $3d^9\ ^2D$.[18] However, to the best of our knowledge, there is no report about the reactions of the excited states of anions.

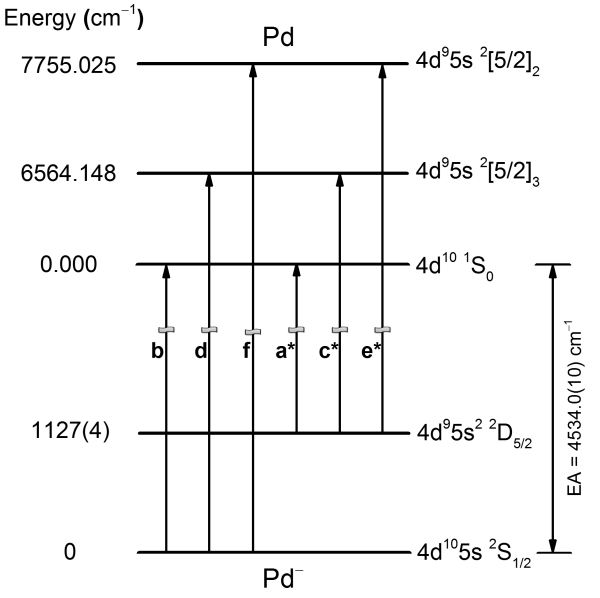

Figure 1. Energy levels of Pd and Pd^- related to the present experiment. The labels of photodetachment channels indicate the peaks in the energy spectra in Figure 2.

Received: December 27, 2018
Accepted: January 30, 2019
Published: January 30, 2019

DOI: 10.1021/acs.jpclett.8b03859
J. Phys. Chem. Lett. 2019, 10, 702−706

We use our newly constructed photoelectron energy spectrometer equipped with a cold octupole radio frequency (rf) ion trap to study the reaction of Pd^- with H_2. The main features of this apparatus are the high-energy resolution of the slow-electron velocity-map imaging technique, typically a few cm^{-1},[24−26] and the cold ion trap with a controlled temperature in the range of 5−300 K.[27] The detailed description of the spectrometer can be found elsewhere.[28] The Pd anions are produced via the pulsed YAG laser ablation of the Pd metal disk. Then, the generated anions are accumulated and stored in the ion trap.[24,29] Because the transition from the excited state $4d^95s^2\ ^2D_{5/2}$ to the ground state $4d^{10}5s\ ^2S_{1/2}$ is parity forbidden, the excited state $^2D_{5/2}$ has a very long lifetime. In the ion trap, the Pd anions collide and react with H_2 gas. The pressure of H_2 gas and the reaction time can be carefully controlled. The charged products can be observed via the time-of-flight mass spectrometry.[30] In addition, the electronic states of the anions of interest can be characterized via the high-resolution photoelectron spectroscopy based on the velocity mapping imaging technique.[31,32] The spectrometer runs at a 20 Hz repetition rate.

The mixture of 20% H_2 and 80% He gas is routinely used as buffer cooling gas in our experiment. The mixture gas is injected into the ion trap via a pulsed valve. The trapped Pd^- anions collide and react with H_2 gas during the trapping period, which can be adjusted from 5 to 45 ms. Pure He gas (≥99.999%) is also used for the purpose of comparison. Figure 2 shows the energy spectra of Pd^- confined in the ion trap for 45 ms using different gases at the temperature 300 K. As shown in Figure 2a, six peaks labeled with a*, b, c*, d, e*, and f were observed when the pure He gas was used as the buffer gas. The peaks b, d, and f are transitions from the ground state $4d^{10}5s\ ^2S_{1/2}$ of Pd^- anion, and a*, c*, and e* are from the excited state $4d^95s^2\ ^2D_{5/2}$ of Pd^-, as illustrated in Figure 1. When the gas 20% H_2 + 80% He was used instead of the pure He gas, we observed that peaks b, d, and f almost disappeared. It is a surprising result because the three peaks are all from the ground state of Pd^-. For other anionic species, we usually observe an enhancement of the peaks photodetached from the ground state because the population in the ground state will increase because of the de-excitation of excited states. Why does the population at the ground state become significantly less? The only possible explanation is that the ground-state Pd^- reacts with H_2 much faster than the excited-state Pd^-. It is unusual because the excited states are often more reactive than the ground state. To confirm the explanation, we also measured the mass spectrum after the reaction. The signal of PdH^- was observed when the gas 20% H_2 + 80% He was used, while the PdH^- signal was absent when the pure He gas was used. This indicated that Pd^- indeed reacts with H_2.

In contrast, methane gas, CH_4, was used as the buffer gas to quench the excited state. We found that CH_4 can effectively quench the excited state of Pd^- because the vibrational frequency of its asymmetric bend mode 1306 cm^{-1} is close to the excitation energy of Pd^- (1127.0(40) cm^{-1}).[33] The buffer gas we used was a mixture of 5% CH_4 and 95% He. As shown in Figure 2b, the intensities of peaks a*, c*, and e* from the excited state were significantly suppressed. The intensity decreased to ∼1/6 of that as the pure He gas was used. The excited state $4d^95s^2\ ^2D_{5/2}$ of Pd^- has a much longer lifetime than the typical trap time because of the forbidden transition. Because the population does not change during the trap time when using the He gas, the relative population on the excited

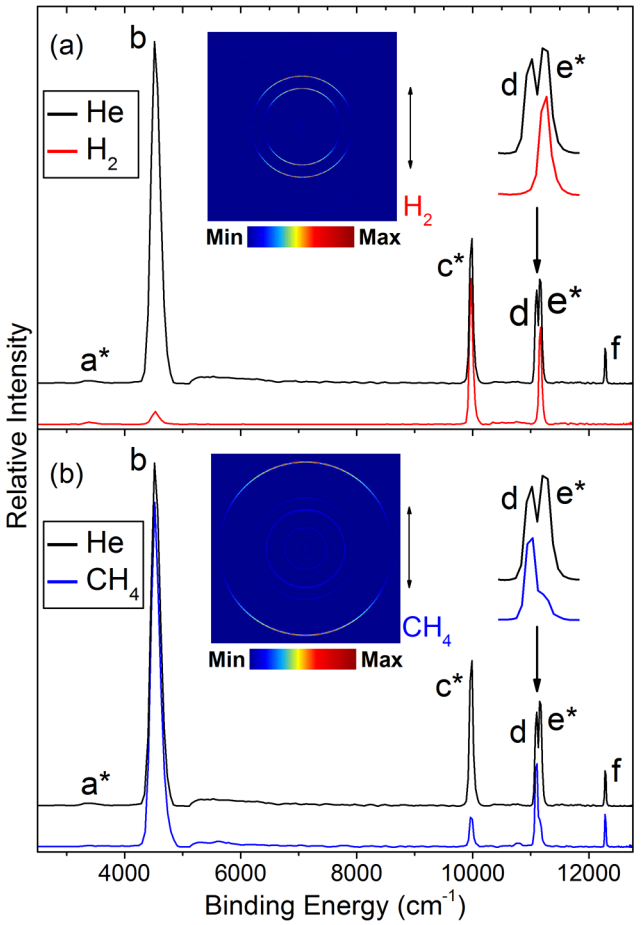

Figure 2. Photoelectron energy spectra of Pd^- at the photon energy $h\nu$ = 12 760 cm^{-1}. The reaction gases are (a) 20% H_2 + 80% He and (b) 5% CH_4 + 95% He. The energy spectra using the pure He gas are also plotted for comparison. The insets show the photoelectron velocity images. The double arrows indicate the laser polarization. For a clear view, peaks d and e* were expanded in the insets.

state is ∼30% according to a Boltzmann distribution for the ion source.[27,34] The relative population of the excited state becomes 5% after the trap when CH_4 gas is used as the buffer gas. In fact, the gas density in the trap exponentially decays after the pulsed injection (see Figure S1 in the Supporting Information). It is found that most of the quench processes happen during the first 5 ms during the trap. It does not need to trap Pd^- anions for 45 ms. Therefore, with the help of CH_4, we can prepare Pd^- anions with a population of 95% at the ground state.

To measure the reaction rate constant of Pd^- with H_2 at room temperature (300 K), we need to thermalize hot Pd^- anions to room temperature. The kinetic energy of the Pd^- anions can be as high as a few electronvolts because the laser ablation ion source works in the free-jet mode in the present experiment. Two pulsed valves are used to deliver the buffer gas and the reaction gas separately. The first valve delivers a pulse of buffer gas (He or CH_4) when the ions enter the ion trap. It is found that 5 ms is enough to thermalize the Pd^- to 300 K through collisions with buffer gas. Then, the second valve delivers a pulse of the reaction gas (H_2). To measure the partial pressure of H_2 in the ion trap, we use the well-known reaction $O^- + H_2 \rightarrow OH^- + H$ to do the calibration.[35,36] The reaction rate constant can be determined by measuring the

DOI: 10.1021/acs.jpclett.8b03859
J. Phys. Chem. Lett. 2019, 10, 702−706

intensity of related anions using the time-of-flight mass spectrometry (see Figures S2–S4 in the Supporting Information).

In the preliminary measurement, we found that there are two stages in the reaction of Pd^- with H_2 when the pure He is used as buffer gas. In the first stage, the intensity of Pd^- decreases very fast, but the intensity of PdH^- does not increase correspondingly. The intensity of Pd^- quickly decays to one-tenth of its original value as H_2 gas pressure increased from 0 to 0.1 Pa. In the second stage (>0.1 Pa), the intensity of PdH^- increases correspondingly as the Pd^- decreases gradually when more H_2 gas is delivered into the ion trap. This observation shows that there are two different reactions between Pd^- and H_2, and their reaction rates are significantly different. As shown in Figure 3a, the relative intensity of Pd^- correlates closely with

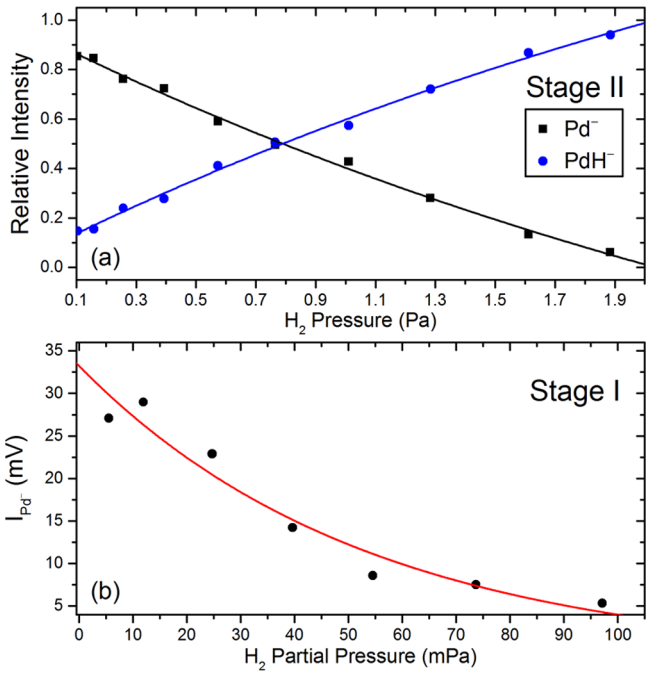

Figure 3. Relative intensities of Pd^- and PdH^- after the excited Pd^- reacts with H_2 in the ion trap for 13 ms (a); signal intensity of Pd^- after the ground-state Pd^- reacts with H_2 (b).

that of PdH^- as the pressure of H_2 increases. From the photoelectron energy spectrum, we know that the ground-state Pd^- anions are mainly depleted in the first stage. Therefore, it can be concluded that the reaction channel in stage II is

$$Pd^-(^2D_{5/2}) + H_2 \rightarrow PdH^- + H \quad (1)$$

In stage I, no charged products related to the reaction of Pd^- + H_2 were observed in the mass spectrometry. It is reasonable to assume that the product is a neutral species. According to the calculations using the CCSD(T) method with the aug-cc-pVTZ basis set, the total energy of PdH_2 is lower than that of PdH + H. Therefore, we conjecture that the reaction in stage I is

$$Pd^-(^2S_{1/2}) + H_2 \rightarrow PdH_2 + e^- \quad (2)$$

At the current stage, the direct observation of the neutral product PdH_2 is beyond our ability because of the extremely high sensitivity and selectivity required for trace detection. Because the ground-state Pd^- has been almost completely depleted in stage I, it is the excited Pd^- anions that react with H_2 in reaction 1 for producing PdH^-. The pseudo-first-order rate constant of reaction 1 is determined to be 5.2×10^{-12} $cm^3\ s^{-1}$ by measuring the relative intensity of Pd^- and PdH^-.[37] In order to measure the rate of the reaction 2, it is better to prepare Pd^- at its ground state. This can be realized by using 5% CH_4 + 95% He as the buffer gas, as mentioned previously. Considering the reaction 2 is rather rapid, the diluted H_2 gas (20% H_2 + 80% He) was used. The intensity of Pd^- versus the H_2 partial pressure is shown in Figure 3b. The reaction rate constant is measured to be 7.6×10^{-11} $cm^3\ s^{-1}$, which is about ten times greater than that of the reaction 1. It should be noted that the temperature of trapped ions may be slightly higher than the nominal temperature because of rf heating.[38−40]

To answer why the ground-state Pd^- reacts with H_2 much faster than the excited Pd^-, we calculated the potential energy curves as H_2 approaches Pd^- head to head using the multireference configuration interaction (MRCI) method with the aug-cc-pVTZ basis set. The single-point energies were calculated at the CCSD(T)/aug-cc-pVTZ level. Figure 4

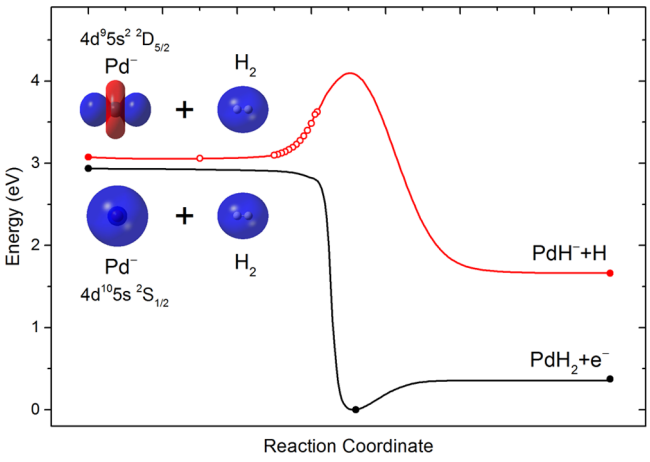

Figure 4. Schematic potential energy curves for the reactions of Pd^- at the excited state $^2D_{5/2}$ (red) and the ground state $^2S_{1/2}$ (black) with H_2. The solid dots indicate the energies are obtained using the CCSD(T) method, while the empty dots indicate MRCI. The contours are the frontier molecular orbitals of Pd^- and H_2.

illustrates the schematic reaction paths for reactions 1 and 2. Because of the different orbital symmetries, the reaction of excited state $Pd^-(^2D_{5/2})$ + H_2 has a high barrier, while there is no barrier for the ground-state $Pd^-(^2S_{1/2})$ + H_2. This explains why the ground-state Pd^- reacts much faster with H_2 than the excited Pd^-. The energy spectrum of the product PdH^- was also measured, as shown in Figure S5 of the Supporting Information. The electron affinity of PdH is 10 759(100) cm^{-1}, and the vibrational frequency is 1967(135) cm^{-1}.

In conclusion, the high-resolution photoelectron energy spectra in combination with the mass spectrometry results clearly show that the ground-state Pd^- anions react with H_2 much faster than the excited state Pd^- anions. This is the first time such an effect has been observed for the state-specific reaction of anions. As demonstrated in the present work, the combination of the ion trap and the high-resolution photoelectron velocity-mapping imaging provides a new tool for exploring the kinetics and dynamics of chemical reactions involving negative ions.

DOI: 10.1021/acs.jpclett.8b03859
J. Phys. Chem. Lett. 2019, 10, 702−706

■ ASSOCIATED CONTENT

Supporting Information

The Supporting Information is available free of charge on the ACS Publications website at DOI: 10.1021/acs.jpclett.8b03859.

Detailed experimental method for measuring the reaction rate constants, simulations of gas pressure evolution in the ion trap, typical mass spectra, and the photoelectron energy spectrum of PdH^- (PDF)

■ AUTHOR INFORMATION

Corresponding Author

*E-mail: ningcg@tsinghua.edu.cn.

ORCID

Chuangang Ning: 0000-0002-3158-1253

Notes

The authors declare no competing financial interest.

■ ACKNOWLEDGMENTS

This work is supported by the National Natural Science Foundation of China (NSFC) (Grant No. 91736102) and the National Key R&D program of China (2018YFA0306504).

■ REFERENCES

(1) Adams, B. D.; Chen, A. The Role of Palladium in a Hydrogen Economy. *Mater. Today* **2011**, *14*, 282−289.

(2) Wolf, R.; Mansour, K. The Amazing Metal Sponge: Soaking Up Hydrogen. *Projects in Scientific Computing*, **1995**.

(3) Park, E. D.; Lee, D.; Lee, H. C. Recent Progress in Selective CO Removal in a H_2-Rich Stream. *Catal. Today* **2009**, *139*, 280−290.

(4) Kamakoti, P.; Morreale, B. D.; Ciocco, M. V.; Howard, B. H.; Killmeyer, R. P.; Cugini, A. V.; Sholl, D. S. Prediction of Hydrogen Flux Through Sulfur-Tolerant Binary Alloy Membranes. *Science* **2005**, *307*, 569−573.

(5) Narehood, D. G.; Kishore, S.; Goto, H.; Adair, J. H.; Nelson, J. A.; Gutiérrez, H. R.; Eklund, P. C. X-Ray Diffraction and H-Storage in Ultra-Small Palladium Particles. *Int. J. Hydrogen Energy* **2009**, *34*, 952−960.

(6) Antolini, E. Palladium in Fuel Cell Catalysis. *Energy Environ. Sci.* **2009**, *2*, 915.

(7) Griessen, R.; Strohfeldt, N.; Giessen, H. Thermodynamics of the Hybrid Interaction of Hydrogen with Palladium Nanoparticles. *Nat. Mater.* **2016**, *15*, 311−317.

(8) Narayan, T. C.; Hayee, F.; Baldi, A.; Leen Koh, A.; Sinclair, R.; Dionne, J. A. Direct Visualization of Hydrogen Absorption Dynamics in Individual Palladium Nanoparticles. *Nat. Commun.* **2017**, *8*, 14020.

(9) Yamauchi, M.; Ikeda, R.; Kitagawa, H.; Takata, M. Nanosize Effects on Hydrogen Storage in Palladium. *J. Phys. Chem. C* **2008**, *112*, 3294−3299.

(10) Andersen, T.; Haugen, H. K.; Hotop, H. Binding Energies in Atomic Negative Ions: III. *J. Phys. Chem. Ref. Data* **1999**, *28*, 1511−1533.

(11) Scheer, M.; Brodie, C. A.; Bilodeau, R. C.; Haugen, H. K. Laser Spectroscopic Measurements of Binding Energies and Fine-Structure Splittings of Co^-,Ni^-,Rh^-,and Pd^-. *Phys. Rev. A: At., Mol., Opt. Phys.* **1998**, *58*, 2051−2062.

(12) Elkind, J. L.; Armentrout, P. B. Effect of Kinetic and Electronic Energy on the Reactions of Cr^+ with H_2, HD, and D 2. *J. Chem. Phys.* **1987**, *86*, 1868−1877.

(13) Hanton, S. D.; Noll, R. J.; Weisshaar, J. C. Spin-Orbit-Level Effect on $Fe^+(3d^7,{}^4F_J)$ + C_3H_8 Total Reaction Cross Section at 0.22 eV. *J. Phys. Chem.* **1990**, *94*, 5655−5658.

(14) Zhang, T.; Qian, X. M.; Tang, X. N.; Ng, C. Y.; Chiu, Y.; Levandier, D. J.; Miller, J. S.; Dressler, R. A. A State-Selected Study of the $H_2^+(X,v^+=0-17,N^+=1)$+Ne Proton Transfer Reaction Using the Pulsed-Field Ionization−Photoelectron−Secondary Ion Coincidence Scheme. *J. Chem. Phys.* **2003**, *119*, 10175−10185.

(15) Armentrout, P. B. Electronic State-Specific Transition Metal Ion Chemistry. *Annu. Rev. Phys. Chem.* **1990**, *41*, 313−344.

(16) Armentrout, P. B. Chemistry of Excited Electronic States. *Science* **1991**, *251*, 175−179.

(17) Clemmer, D. E.; Chen, Y.-M.; Khan, F. A.; Armentrout, P. B. State-Specific Reactions of $Fe^+(a^6D,a^4F)$ with D_2O and Reactions of FeO^+ with D_2. *J. Phys. Chem.* **1994**, *98*, 6522−6529.

(18) Elkind, J. L.; Armentrout, P. B. Effect of Kinetic and Electronic Energy on the Reactions of Co^+, Ni^+, and Cu^+ with H_2, HD, and D_2. *J. Phys. Chem.* **1986**, *90*, 6576−6586.

(19) Ng, C.-Y. State-Selected and State-to-State Ion−Molecule Reaction Dynamics. *J. Phys. Chem. A* **2002**, *106*, 5953−5966.

(20) Li, X.; Huang, Y. L.; Flesch, G. D.; Ng, C. Y. Absolute State-Selected Total Cross Sections for the Ion−Molecule Reactions $O^+(^4S,^2D,^2P)$+$H_2(D_2)$. *J. Chem. Phys.* **1997**, *106*, 564−571.

(21) Li, X.; Huang, Y. L.; Flesch, G. D.; Ng, C. Y. A State-Selected Study of the Ion−Molecule Reactions $O^+(^4S,^2D,^2P)$+N_2. *J. Chem. Phys.* **1997**, *106*, 1373−1381.

(22) Georgiadis, R.; Armentrout, P. B. Translational and Electronic Energy Dependence of Chromium Ion Reactions with Methane. *J. Phys. Chem.* **1988**, *92*, 7067−7074.

(23) Flesch, G. D.; Ng, C. Y. Absolute State-Selected and State-to-State Total Cross Sections for the Ar $^+(^2P_{3/2,1/2})$+CO_2 reactions. *J. Chem. Phys.* **1992**, *97*, 162−172.

(24) Weichman, M. L.; Neumark, D. M. Slow Photoelectron Velocity-Map Imaging of Cryogenically Cooled Anions. *Annu. Rev. Phys. Chem.* **2018**, *69*, 101−124.

(25) Luo, Z. H.; Chen, X. L.; Li, J. M.; Ning, C. G. Precision Measurement of the Electron Affinity of Niobium. *Phys. Rev. A: At., Mol., Opt. Phys.* **2016**, *93*, No. 020501, (R). .

(26) Chen, X. L.; Ning, C. G. Observation of Rhenium Anion and Electron Affinity of Re. *J. Phys. Chem. Lett.* **2017**, *8*, 2735−2738.

(27) Tang, R. L.; Chen, X. L.; Fu, X. X.; Wang, H.; Ning, C. G. Electron Affinity of the Hafnium Atom. *Phys. Rev. A: At., Mol., Opt. Phys.* **2018**, *98*, No. 020501, (R). .

(28) Tang, R. L.; Fu, X. X.; Ning, C. G. Accurate Electron Affinity of Ti and Fine Structures of Its Anions. *J. Chem. Phys.* **2018**, *149*, 134304.

(29) Wang, X. B.; Wang, L. S. Development of a Low-Temperature Photoelectron Spectroscopy Instrument Using an Electrospray Ion Source and a Cryogenically Controlled Ion Trap. *Rev. Sci. Instrum.* **2008**, *79*, No. 073108.

(30) Wiley, W. C.; McLaren, I. H. Time-of-Flight Mass Spectrometer with Improved Resolution. *Rev. Sci. Instrum.* **1955**, *26*, 1150−1157.

(31) León, I.; Yang, Z.; Liu, H. T.; Wang, L. S. The Design and Construction of a High-Resolution Velocity-Map Imaging Apparatus for Photoelectron Spectroscopy Studies of Size-Selected Clusters. *Rev. Sci. Instrum.* **2014**, *85*, No. 083106.

(32) Eppink, A. T. J. B.; Parker, D. H. Velocity Map Imaging of Ions and Electrons Using Electrostatic Lenses: Application in Photoelectron and Photofragment Ion Imaging of Molecular Oxygen. *Rev. Sci. Instrum.* **1997**, *68*, 3477−3484.

(33) Herzberg, G. *Molecular Spectra and Molecular Structure*; Van Nostrand Company, Inc: Princeton, NJ, 1966.

(34) Chen, X. L.; Ning, C. G. Accurate Electron Affinity of Co^- and Fine-Structure Splittings of Co−via Slow-Electron Velocity-Map Imaging. *Phys. Rev. A: At., Mol., Opt. Phys.* **2016**, *93*, No. 052508.

(35) Jusko, P.; Roučka, Š; Mulin, D.; Zymak, I.; Plašil, R.; Gerlich, D.; Cížek, M.; Houfek, K.; Glosík, J. Interaction of O^- and H_2 at Low Temperatures. *J. Chem. Phys.* **2015**, *142*, No. 014304.

(36) Jusko, P.; Roučka, Š; Plašil, R.; Glosík, J. Determining the Energy Distribution of Electrons Produced in Associative Detachment: the Electron Spectrometer with Multipole Trap. *Int. J. Mass Spectrom.* **2013**, *352*, 19−28.

(37) Yuan, Z.; Li, Z. Y.; Zhou, Z. X.; Liu, Q. Y.; Zhao, Y. X.; He, S. G. Thermal Reactions of $(V_2O_5)_nO^-$(n= 1−3) Cluster Anions with

DOI: 10.1021/acs.jpclett.8b03859
J. Phys. Chem. Lett. 2019, 10, 702−706

Ethylene and Propylene: Oxygen Atom Transfer Versus Molecular Association. *J. Phys. Chem. C* **2014**, *118*, 14967−14976.
(38) Liu, H. T.; Ning, C. G.; Huang, D.-L.; Wang, L. S. Vibrational Spectroscopy of the Dehydrogenated Uracil Radical by Autodetachment of Dipole-Bound Excited States of Cold Anions. *Angew. Chem.* **2014**, *53126*, 2496−2500.
(39) Wester, R. Radiofrequency Multipole Traps: Tools for Spectroscopy and Dynamics of Cold Molecular Ions. *J. Phys. B: At., Mol. Opt. Phys.* **2009**, *42*, 154001.
(40) Hock, C.; Kim, J. B.; Weichman, M. L.; Yacovitch, T. I.; Neumark, D. M. Slow Photoelectron Velocity-Map Imaging Spectroscopy of Cold Negative Ions. *J. Chem. Phys.* **2012**, *137*, 244201.

DOI: 10.1021/acs.jpclett.8b03859
J. Phys. Chem. Lett. 2019, 10, 702−706